Published in final edited form as:
Chem Res Toxicol. 2008 May ; 21(5): 1056–1063. doi:10.1021/tx800056w.

Pristine (C_{60}) and Hydroxylated [$C_{60}(OH)_{24}$] Fullerene Phototoxicity towards HaCaT Keratinocytes:

Type I vs Type II Mechanisms

Baozhong Zhao*, **Yu-Ying He**, **Piotr J. Bilski**, and **Colin F. Chignell**
Laboratory of Pharmacology and Chemistry, National Institute of Environmental Health Sciences, Research Triangle Park, North Carolina 27709

Abstract

The increasing use of fullerene nanomaterials has prompted widespread concern over their biological effects. Herein, we have studied the phototoxicity of γ-cyclodextrin bicapped pristine C_{60} [(γ-CyD)$_2$/C_{60}] and its water-soluble derivative $C_{60}(OH)_{24}$ toward human keratinocytes. Our results demonstrated that irradiation of (γ-CyD)$_2$/C_{60} or $C_{60}(OH)_{24}$ in D_2O generated singlet oxygen with quantum yields of 0.76 and 0.08, respectively. Irradiation (>400 nm) of $C_{60}(OH)_{24}$ generated superoxide as detected by the EPR spin trapping technique; superoxide generation was enhanced by addition of the electron donor nicotinamide adenine dinucleotide (reduced) (NADH). During the irradiation of (γ-CyD)$_2$/C_{60}, superoxide was generated only in the presence of NADH. Cell viability measurements demonstrated that (γ-CyD)$_2$/C_{60} was about 60 times more phototoxic to human keratinocytes than $C_{60}(OH)_{24}$. UVA irradiation of human keratinocytes in the presence of (γ-CyD)$_2$/C_{60} resulted in a significant rise in intracellular protein-derived peroxides, suggesting a type II mechanism for phototoxicity. UVA irradiation of human keratinocytes in the presence of $C_{60}(OH)_{24}$ produced diffuse intracellular fluorescence when the hydrogen peroxide probe Peroxyfluor-1 was present, suggesting a type I mechanism. Our results clearly show that the phototoxicity induced by (γ-CyD)$_2$/C_{60} is mainly mediated by singlet oxygen with a minor contribution from superoxide, while $C_{60}(OH)_{24}$ phototoxicity is mainly due to superoxide.

Introduction

Nanotechnology is currently an area of intense scientific interest, due to the many potential applications in the biomedical, optical, and electronic fields. Nanomaterials encompass a wide variety of chemical structures including fullerenes, nanotubes, dendrimers, and quantum dots. The increasing use of nanomaterials has prompted widespread concern over their safety. Buckministerfullerenes (fullerenes) are a class of carbon nanomaterials with biomedical, electronic, and semiconductor applications (1-4). The potential environmental and health effects of fullerenes have attracted increasing attention in recent years (5-8), especially with the development of water-soluble forms that facilitate their use in biological systems (3,9).

The unique electronic π-system of fullerenes makes them potential photosensitizers upon the absorption of UV or visible light. Our previous studies (10) have shown that a variety of water-soluble fullerenes can efficiently generate singlet oxygen ($^1O_2$) upon irradiation via energy transfer (type II photochemical mechanism) from the excited triplet of fullerene to oxygen (11-13). There are also reports that photoirradiation of fullerenes in aqueous systems results in the production of the corresponding radical anions ($C_{60}^{\cdot-}$) followed by generation of

*To whom correspondence should be addressed. Fax: +1-919-541-5750. E-mail: zhaob2@niehs.nih.gov.

superoxide ($O_2^{\cdot-}$) and hydroxyl radical ($^{\cdot}OH$) via electron transfer (type I photochemical mechanism), especially in the presence of electron donors (such as NADH or amines) (14-18). These two photochemical mechanisms, typically present during photodynamic therapy (PDT), constitute the main pathways for the photoinduced toxicity of fullerenes (19).

The poor solubility of pristine, underivatized fullerene (C_{60}) in water has so far greatly hindered the investigation of its biological properties. To overcome this, a C_{60} water suspension can be prepared by means of solvent replacement (20,21), sonication (22), addition of artificial/natural surfactants (23-26), or simply by stirring over time (27); these procedures result in the formation of water-stable C_{60} aggregates. However, our previous studies (10), as well as some recent reports, have demonstrated a marked decrease or complete loss of photoreactivity of the aggregated forms (8,27). C_{60} can also be solubilized in water by using γ-cyclodextrin (γ-CyD) as a host to form a complex wherein the C_{60} is encapsulated between the cavities of two γ-CyD molecules (28-30). Aqueous solubility can also be achieved by chemically modifying or functionalizing the C_{60} surface with hydrophilic substituents, such as hydroxyl (31), carboxyl (32), quaternary ammonium (33), diamido diacid diphenyl (34), or poly(ethylene glycol) (35) groups.

An understanding of the phototoxicity and photochemical mechanisms of fullerene nanomaterials is important for biomedical applications as well as environmental and health evaluation. We herein report the phototoxic effects on human keratinocytes induced by γ-CyD bicapped pristine C_{60} in comparison with its water-soluble derivative $C_{60}(OH)_{24}$. In addition, we have measured and compared their generation of singlet oxygen and superoxide radical and carried out in vitro experiments to elucidate the unique mechanisms for their individual phototoxicity.

Materials and Methods

Chemicals

C_{60} (99.9%, sublimed), γ-cyclodextrin (99.0%), dimethylsulfoxide (DMSO,[1] cell-culture grade), nicotinamide adenine dinucleotide (reduced) (NADH), and catalase (27 mg protein/mL, 47000 units/mg protein) were all purchased from Sigma-Aldrich, Inc. (St. Louis, MO). 5,5-Dimethyl-1-pyrroline *N*-oxide (DMPO) (Aldrich Chemical Co., Milwaukee, WI) was vacuum distilled and stored at -70 °C until use. $C_{60}(OH)_{24}$ was supplied by Battelle Columbus (Columbus, OH). PF-1 was synthesized by the procedure of Chang et al. (36).

Preparation of γ-Cyclodextrin Bicapped C_{60} [$(\gamma\text{-CyD})_2/C_{60}$] and $C_{60}(OH)_{24}$ Solution

γ-Cyclodextrin bicapped C_{60} [$(\gamma\text{-CyD})_2/C_{60}$] was prepared by the method of Yoshida et al. (28,29) with some modification. Briefly, a mixture of C_{60} (40.0 mg; 55.6 μmol) and γ-cyclodextrin (120.0 mg; 92.5 μmol) was stirred in a water/toluene (16/6 v/v) mixture at 118 °C for 48 h, and then, γ-cyclodextrin (60.0 mg; 46.3 μmol) was added twice more at 48 h intervals. After the mixture was cooled to room temperature (RT), the aqueous layer containing precipitated $(\gamma\text{-CyD})_2/C_{60}$ was vacuum filtered through a 0.22 μm nylon membrane. The purple crystals were washed with methanol to remove any free γ-cyclodextrin and were dried in vacuo. To obtain a concentrated $(\gamma\text{-CyD})_2/C_{60}$ water solution, 3.5 mg of the solid was added to 5 mL of ultrapure water and heated at 85 °C for about 5 min until a clear solution formed. Then, the solution was filtered/sterilized through a 0.22 μm cellulose acetate membrane to remove the insoluble materials (C_{60} released from unstable complexes) and bacteria. The concentration of the solution was determined from its absorbance at 332 nm [log ε = 4.63 (29)]. This solution was prepared fresh before each use because the complex was unstable in water.

The $C_{60}(OH)_{24}$ solution was prepared by first dissolving it in DMSO to produce a 5 mM stock solution and then diluting according to the requirements of the experiments. The maximum DMSO concentration for $C_{60}(OH)_{24}$ (50 μM) solution was 1% (v/v).

Absorption and Singlet Oxygen Phosphorescence Emission Spectra

All absorption spectra were recorded on a Hewlett-Packard diode array spectrophotometer model 8452A (Hewlett-Packard Co., Palo Alto, CA). Singlet oxygen phosphorescence was recorded on a steady-state $^1O_2$ spectrophotometer (37) featuring an optimized optical system as in our pulse $^1O_2$ spectrophotometer (38). Samples were excited with a 500 W mercury lamp operating at 300 W through a filter with maximal transmittance at 366 nm. The $^1O_2$ phosphorescence spectra were recorded over the range 1200-1350 nm and were normalized to the same number of absorbed photons (39) at the excitation wavelength.

Cell Viability

HaCaT keratinocytes, a transformed epidermal human cell line (40), were grown at 37 °C in Dulbecco's modified Eagle's medium (DMEM) containing 10% fetal bovine serum (FBS) to ~95% confluence in 96 well plates in an atmosphere of 95% air/5% CO_2. For photocytotoxicity tests, cells were exposed in the dark for 2 h at 37 °C to different fullerenes in DMEM (FBS free). Control cells were treated with DMEM alone. After incubation, the medium was removed

---

[1]Abbreviations:

BSA bovine serum albumin

DMEM Dulbecco's modified Eagle's medium

DMPO 5,5-dimethy-1-pyrroline *N*-oxide

DMSO dimethylsulfoxide

EPR electron paramagnetic resonance

FBS fetal bovine serum

MTS 3-(4,5-dimethylthiazol-2-yl)-5-(3-carboxymethoxyphenyl)-2-(4-sulfophenyl)-2H-tetrazolium

NADH nicotinamide adenine dinucleotide (reduced)

PBS phosphate buffered saline

PF1 peroxyfluor-1

POOH protein hydroperoxide

ROS reactive oxygen species

RT room temperature

UVA ultraviolet A (315-400 nm)

and replaced by sterile phosphate-buffered saline (PBS) containing 10 mM glucose. Cells were then irradiated with ultraviolet A (UVA) from four fluorescent PUVA lamps (Houvalite F20T12BL-HO; National Biological Co. Twinsburg, OH) or cool white visible light (Phillips F40 AX50, 5000 K Advantage). The fluences were 15 and 5.4 J/cm^2, respectively, as measured with a YSI-Kettering model 65A Radiometer (Yellow Springs Instrument Co., Yellow Springs, OH). After exposure, the PBS/glucose solution was removed and replaced with DMEM containing 2% FBS, and the cells were kept in the incubator for 16 h. The medium was removed, and the cells were washed with PBS and then treated with 100 μL/well of PBS/glucose containingthe3-(4,5-dimethylthiazol-2-yl)-5-(3-carboxymethoxyphenyl)-2-(4-sulfophenyl)-2H-tetrazolium (MTS) reagent (Cell-Titer 96 Aqueous Proliferation Assay; Promega Corp.). After incubation for 2 h at 37 °C, the absorbance at 492 nm was recorded using a microplate reader (Spectrafluor Plus, Tecan US, Research Triangle Park, NC).

Cell Uptake of Fullerenes

HaCaT cells were grown in 100 mm × 20 mm dishes to ~90% confluence at 37 °C in DMEM containing 10% FBS in an atmosphere of 95% air/5% CO_2. The medium was removed, and the cells were washed with PBS and then incubated with DMEM (FBS free) containing 50 μM fullerene. After incubation, the medium was removed, and the cells were washed twice with PBS. The cells were then scraped, collected into a 15 mL tube, and spun down. The cells were diluted into 1 mL of water and transferred into a 1.5 mL tube. Each sample was sonicated using an Ultrasonic Homogenizer (Cole-Parmer, 4710 series) for 15 s and then centrifuged at 20000*g* for 10 min at 4 °C. The protein concentration was determined by using the BCA assay (Pierce, Rockford, CA). The fullerene concentration was estimated from the absorption spectra of the solution. The peak absorbance at 332 nm was compared to a standard curve prepared by addition of varying amounts of fullerenes in bovine serum albumin (BSA) solution (the concentration of BSA was adjusted to be approximately the same in each solution, with the protein concentration obtained by BCA assay). Note that this method does not discriminate between fullerenes bound to the cell membranes and those that are fully internalized.

Electron Paramagnetic Resonance (EPR) Spectra

EPR spectra were recorded using a Varian E-109 Century line spectrometer (Varian Associates, Palo Alto, CA) operating at 9.78 GHz with 100 kHz modulation. All EPR spectra were recorded at RT in a quartz flat cell on a Bruker EMX EPR spectrometer equipped with a super high-Q cavity (Bruker, Billerica, MA). Spectra were recorded using an IBM-compatible computer interfaced with the spectrometer with the following instrument settings and conditions: 10 mW microwave power, 100 kHz modulation frequency, 1 G modulation amplitude, 655 ms time constant, 335 s scan time, and a single scan of 100 G. Where indicated, samples were placed in a quartz flat cell and irradiated directly inside the microwave cavity of the spectrometer using a 1 kW Xe arc lamp. Radiation from the lamp was passed through a 30 mm path length liquid filter [aqueous solution containing (in g/L) $NaNO_2$, 48.4; Na_2CO_3, 1; and K_2CrO_4, 0.2] to remove wavelengths below 400 nm or a glass filter to remove wavelengths below 300 nm.

Oxygen Consumption

Oxygen consumption was measured using a Clark oxygen electrode (Yellow Springs Instruments). Aqueous solutions of (γ-CyD)$_2$/C_{60} or $C_{60}(OH)_{24}$ in a water-jacketed cell (2 mL total volume) were irradiated using a Xe arc lamp, and the oxygen consumption was measured in the absence or presence of 2 mM histidine or NADH (singlet oxygen substrates) with or without 10 mM sodium azide (singlet oxygen quencher). In the case of NADH, oxygen evolution was detected upon the addition of 50 μg/mL catalase. When samples containing NADH were irradiated, radiation from the lamp was passed through a 30 mm path length liquid

filter [an aqueous solution containing (in g/L) $NaNO_2$, 48.4; Na_2CO_3, 1; and K_2CrO_4, 0.2] to remove wavelengths below 400 nm.

Measurement of Protein Peroxides

To measure protein peroxides, HaCaT cells were suspended in PBS, and 2 mL aliquots containing 8×10^6 cells were placed in individual wells of a six well plate (Becton Dickinson, Franklin Lakes, NJ). After the addition of 10 μM (γ-CyD)$_2$/C_{60} or $C_{60}(OH)_{24}$, the cells were incubated at 37 °C for 2 h and then exposed to UVA radiation as described above for 20 min. Control cells either contained no fullerenes or were kept in the dark. Where indicated, sodium azide (10 mM) was present during treatment. Intracellular protein peroxides were assayed using a modified FOX assay as described by Wright et al. (41). The absorbance was measured at 560 nm and compared to a standard curve prepared using H_2O_2.

Detection of Hydrogen Peroxide in Living Cells

For detection of H_2O_2 in cells, HaCaT cells were seeded into 35 mm dishes containing a glass coverslip-covered 14 mm cutout (MatTek, Ashland, MA) for live cell microscopy measurement. Cells were incubated with 0.5 μM (γ-CyD)$_2$/C_{60} or 30 μM $C_{60}(OH)_{24}$ for 2 h at 37 °C and then incubated with 5 μM peroxyfluor-1 (PF1) for 5 min in the dark at RT. After treatment, cells were exposed to UVA radiation as described above for 10 min. Control cells either contained no fullerenes or were not exposed to UVA. Confocal fluorescence imaging was performed with a Zeiss LSM-510 META confocal microscope. Excitation was carried out at 488 nm, and emission was collected in a window from 505 to 550 nm.

Results

Characterization of (γ-CyD)$_2$/C_{60} and $C_{60}(OH)_{24}$

It is well-known that pristine fullerene is highly hydrophobic and insoluble in most polar solvents, especially water. We have employed two different fullerene preparations: (i) γ-cyclodextrin bicapped C_{60} [(γ-CyD)$_2$/C_{60}], a noncovalent supermolecular complex, and (ii) $C_{60}(OH)_{24}$, a covalent functionalized hydroxylated C_{60}. Both of these fullerenes are readily soluble in water. However, it has been reported that some functionalized fullerenes may form aggregates in polar media at high concentrations (31,42-45). To verify the formation of aggregates, UV-visible absorption spectra of different concentrations of (γ-CyD)$_2$/C_{60} and $C_{60}(OH)_{24}$ in aqueous solution were recorded. As shown in Figure 1, the absorption of (γ-CyD)$_2$/C_{60} in water showed a linear increase at 332 nm with increasing concentration up to 50 μM (Figure 1A, inset). For the $C_{60}(OH)_{24}$, deviation from the Beer-Lambert law was observed at concentrations of 1 μM and above (Figure 1B, inset). Also, the $C_{60}(OH)_{24}$ absorption maximum was red-shifted from 208 to 224 nm, and an additional broad absorption appeared in the 230-500 nm region with increasing concentration. These results clearly showed that (γ-CyD)$_2$/C_{60} in aqueous solution was present in the monomeric state whereas $C_{60}(OH)_{24}$ became aggregated, possibly due to the formation of a hydrogen bond network (31) as shown in Figure 1D.

Phototoxicity in HaCaT Cells

The phototoxicity of (γ-CyD)$_2$/C_{60} and $C_{60}(OH)_{24}$ toward HaCaT cells was measured using the MTS assay (which mainly measures the activity of mitochondrial dehydrogenases) (Figure 2). No obvious effect on viability was observed when HaCaT cells were exposed to either (γ-CyD)$_2$/C_{60} or $C_{60}(OH)_{24}$ in the dark or to light (UVA and cool white light) alone. However, in the presence of light, both (γ-CyD)$_2$/C_{60} and $C_{60}(OH)_{24}$ caused a concentration-dependent loss of mitochondrial activity. The phototoxicity of (γ-CyD)$_2$/C_{60} was much higher than that of $C_{60}(OH)_{24}$, with IC_{50} values of ~0.25 and ~15 μM, respectively.

Uptake of Fullerenes by HaCaT Cells

The difference in phototoxicity between (γ-CyD)$_2$/C_{60} and $C_{60}(OH)_{24}$ could be due to differential cellular uptake. To test this, the fullerenes were incubated with HaCaT cells in serum-free DMEM culture medium, and their uptake was measured after various exposure times. As shown in Figure 3, the fullerenes rapidly accumulated in the cells in a time-dependent manner, especially during the first 8 h; the uptake of $C_{60}(OH)_{24}$ was much higher than (γ-CyD)$_2$/C_{60}. This result suggests that the lower phototoxicity of $C_{60}(OH)_{24}$ is not due to decreased cell uptake but instead may be due to a difference in photoactivity.

Singlet Oxygen Generation

To examine the generation of singlet oxygen, a major reactive oxygen species (ROS)-mediating photochemical action in biological systems, we used direct detection of $^1O_2$ near-infrared phosphorescence emission at 1270 nm. As shown in Figure 4, the quantum yield of singlet oxygen generation by (γ-CyD)$_2$/C_{60} was nearly 10 times higher than that of $C_{60}(OH)_{24}$, with values of ~0.76 and ~0.08, respectively, in D_2O using perinaphthenone as a reference. The higher singlet oxygen production for (γ-CyD)$_2$/C_{60} as compared with $C_{60}(OH)_{24}$ is consistent with the aforementioned cell viability results. This difference also suggests that the phototoxicity of (γ-CyD)$_2$/C_{60} is most likely mediated by a singlet oxygen (type II) mechanism.

Free Radical Generation: EPR Measurements

EPR spectroscopy in conjunction with spin trapping was used to investigate free radical generation. No signal was found when an aqueous solution of (γ-CyD)$_2$/C_{60} was irradiated (>300 nm) (Figure 5A). However, when NADH was present in the solution [to mimic the strong reducing conditions present in HaCaT cells (46)], irradiation (>300 nm) of (γ-CyD)$_2$/C_{60} generated a strong EPR signal from the $(C_{60})^{\cdot-}$ anion radical (Figure 5B). When DMPO was present, the DMPO/$O_2^{\cdot-}$ adduct was also observed (Figure 5D), confirming the generation of superoxide (15, 17). No signal was found during the irradiation (>400 nm) of NADH alone in the presence of DMPO (data not shown). For $C_{60}(OH)_{24}$ solution, a weak asymmetrical single line (Figure 6A) was generated by irradiation (>300 nm). However, the addition of NADH did not increase but rather decreased the signal intensity. Another difference was that when DMPO was added, the DMPO/$O_2^{\cdot-}$ adduct was observed (Figure 6C) in $C_{60}(OH)_{24}$ solution in the absence of NADH, whereas no such signal was observed for (γ-CyD)$_2$/C_{60} under the same conditions (Figure 5C). After addition of NADH to $C_{60}(OH)_{24}$ solution, the DMPO/$O_2^{\cdot-}$ signal intensity increased accompanied by an additional minor carbon-centered adduct, probably DMPO/$^{\cdot}CH_3$, derived from DMSO (Figure 6D,E). This result clearly shows that more superoxide radical was generated during irradiation of $C_{60}(OH)_{24}$ as compared with (γ-CyD)$_2$/C_{60}, suggesting that the phototoxicity of $C_{60}(OH)_{24}$ is most likely mediated by free radicals (a type I mechanism).

Oxygen Consumption Study

We studied the total oxygen consumption by (γ-CyD)$_2$/C_{60} and $C_{60}(OH)_{24}$ in the absence and presence of histidine or NADH and the quenching effect of added NaN_3. As shown in Figure 7, there was little oxygen consumption when (γ-CyD)$_2$/C_{60} or $C_{60}(OH)_{24}$ was irradiated alone. However, (γ-CyD)$_2$/C_{60} irradiated in the presence of histidine or NADH (2 mM) showed significant oxygen consumption at rates of 236.0 and 141.9 nmol/s, respectively. When the singlet oxygen quencher NaN_3 (10 mM) was present, there was a dramatic reduction in oxygen consumption by about 96 and 79%, respectively. When $C_{60}(OH)_{24}$ was irradiated in the presence of histidine or NADH, oxygen consumption rates were much lower than for (γ-CyD)$_2$/C_{60}, about 21.9 and 24.7 nmol/s, respectively. Quenching by NaN_3 was about 60 and 5%, respectively. In the case of NADH plus NaN_3, oxygen evolution was detected upon the addition of catalase, suggesting that hydrogen peroxide was present.

Intracellular Formation of Protein Peroxides

It is well-known that singlet oxygen can oxidize many biomolecules, including membrane lipids, amino acids, cholesterol, and thiols. Furthermore, proteins are known to be the major intracellular targets for singlet oxygen due to their abundance and fast rates of reaction (41, 47-49). Previous reports have detected the generation of singlet oxygen-mediated protein peroxides in THP-1 and HaCaT cells loaded with Rose Bengal and exposed to visible light using a modified FOX assay (8,41). Here, we used the same assay to measure the formation of protein peroxides in HaCaT cells loaded with fullerenes. As shown in Figure 8, negligible levels of protein peroxides were detected in control cells or in cells that had been preincubated with (γ-CyD)$_2$/C$_{60}$ or C$_{60}$(OH)$_{24}$ and then kept in the dark. Exposure of the control cells to UVA radiation generated 1.64 μM protein peroxides, which increased to 9.78 and 2.38 μM in the presence of 10 μM (γ-CyD)$_2$/C$_{60}$ and C$_{60}$(OH)$_{24}$, respectively. When the singlet oxygen quencher NaN_3 (10 mM) was present during irradiation, the protein peroxide level decreased to 1.46, 2.73, and 1.76 μM, respectively. These data indicate the presence of high levels of singlet oxygen-mediated protein peroxides in HaCaT cells exposed to (γ-CyD)$_2$/C$_{60}$ and UVA radiation. Also, they are consistent with the observed singlet oxygen generation and oxygen consumption results.

Intracellular Generation of Hydrogen Peroxide

Hydrogen peroxide is a major reactive oxygen species in living organisms. Here, we used the intracellular probe PF1 to measure the generation of hydrogen peroxide in cells that had been incubated with fullerenes and irradiated. PF1 exhibits excellent selectivity for H_2O_2 and no photo-oxidation (36); hence, cells can be irradiated in the presence of both PF1 and the fullerenes. Cells were first incubated with 0.5 μM (γ-CyD)$_2$/C$_{60}$ or 30 μM C$_{60}$(OH)$_{24}$ for 2 h at 37 °C. These concentrations were selected because they had similar effects on cell viability. After the addition of PF1 and irradiation with UVA, confocal microscopy of cells incubated with either (γ-CyD)$_2$/C$_{60}$ or C$_{60}$(OH)$_{24}$ showed extensive fluorescence (Figure 9E,F). Cells kept in the dark or exposed to UVA radiation in the absence of (γ-CyD)$_2$/C$_{60}$ or C$_{60}$(OH)$_{24}$ showed no increase in fluorescence (Figure 9A-D). The fluorescence intensity of C$_{60}$(OH)$_{24}$-treated cells was higher than that of (γ-CyD)$_2$/C$_{60}$-exposed cells (Figure 9F vs E). Furthermore, the fluorescence was evenly distributed throughout the cells, which is consistent with generation of highly diffusible hydrogen peroxide during irradiation.

Discussion

The photochemical pathways of the fullerenes reported in this current paper are summarized in Scheme 1. The fullerene molecule is excited by UVA radiation or visible light to form an excited triplet state through intersystem crossing. The fullerene triplet can react directly with oxygen by energy transfer to generate highly reactive singlet oxygen (13), via a type II mechanism. A type I reaction is also possible in which the fullerene triplet is reduced by biological reductants, such as NADH, glutathione, or cysteine, to give the fullerene radical anion. Electron transfer from the latter to oxygen generates the superoxide radical, which dismutates to hydrogen peroxide from which the hydroxyl radical can be formed (14,16,17).

The absorption spectra (Figure 1) confirm that (γ-CyD)$_2$/C$_{60}$ in water was present in a monomeric state whereas C$_{60}$(OH)$_{24}$ was aggregated. It is well-known that aggregation can deactivate the excited electronic states of photosensitizers and cause further loss of photoreactivity. This would explain the observed difference in phototoxicity between (γ-CyD)$_2$/C$_{60}$ and C$_{60}$(OH)$_{24}$, seen in Figure 2. The phototoxicity of monomeric (γ-CyD)$_2$/C$_{60}$ is remarkably high; HaCaT cells were killed at concentrations as low as 0.125 μM when exposed to UVA radiation. In contrast, the phototoxicity of aggregated C$_{60}$(OH)$_{24}$ is ~60 times lower than (γ-CyD)$_2$/C$_{60}$. The uptake of C$_{60}$(OH)$_{24}$ by HaCaT cells is much higher than that

of (γ-CyD)$_2$/C_{60} (Figure 3), which excludes the possibility that lower phototoxicity is due to reduced cellular uptake. Note that the aggregation state of the fullerenes may be rather different in biological fluids and culture media as compared to water and could be further modified upon internalization by cells. However, the lack of a correlation between phototoxicity and cellular uptake for (γ-CyD)$_2$/C_{60}, as well as previous biodistribution studies (44), clearly indicate that $C_{60}(OH)_{24}$ is aggregated both in vivo and in vitro.

Previously, Kamat et al. (50) measured the effects of various scavengers of ROS and buffer deuteration on membrane damage induced by fullerene. These workers claimed that the changes mediated by C_{60} complexed to γ-CyD were predominantly due to singlet oxygen while that caused by $C_{60}(OH)_{18}$ was mainly due to radical species. Our photochemical studies (Figures 4-6) indicate that irradiated fullerenes can generate both singlet oxygen and superoxide in water. However, there are distinct differences between the two fullerenes in the generation of ROS.

Singlet oxygen production by (γ-CyD)$_2$/C_{60}, as measured by phosphorescence emission at 1270 nm, was much higher than that of $C_{60}(OH)_{24}$. The production of superoxide as measured by EPR spin trapping showed that $C_{60}(OH)_{24}$ generated more superoxide than (γ-CyD)$_2$/C_{60}. Oxygen consumption studies are also consistent with the above results. The addition of histidine, a substrate for singlet oxygen, to (γ-CyD)$_2$/C_{60} resulted in the highest oxygen consumption, which was almost completely inhibited by azide. In contrast, oxygen consumption by $C_{60}(OH)_{24}$ was little affected by histidine. It is well-known that NADH can act as both an electron donor for superoxide generation and a substrate for singlet oxygen (51). NADH had similar effects on oxygen consumption by the two fullerene preparations. However, the relative reduction of oxygen consumption by azide was lower, especially for $C_{60}(OH)_{24}$ in the presence of NADH, suggesting that in this case most of the oxygen is transformed into superoxide. These findings are consistent with the hypothesis of Kamat et al. and indicate that (γ-CyD)$_2$/C_{60} operates primarily via a type II reaction, whereas for $C_{60}(OH)_{24}$, a type I reaction is involved.

Singlet oxygen is known to directly react with proteins and unsaturated lipids located in cell membranes to give the corresponding peroxides (Scheme 1). The detection of protein hydroperoxide (POOH) as the major product during photoirradiation of HaCaT cells containing fullerenes and the quenching effect by azide strongly suggest that singlet oxygen is indeed generated inside the cells. Once again, (γ-CyD)$_2$/C_{60} demonstrates a remarkably large increase in protein peroxides via $^1O_2$-mediated reactions. Because the diffusion distance of singlet oxygen is very short [<70 nm (52)], this result also provides indirect evidence that photoreactive fullerene is taken up into cells.

Our intracellular hydrogen peroxide detection further confirms the difference between the phototoxicity of the two fullerenes. It is to be expected that superoxide produced from irradiated fullerenes would undergo dismutation, catalyzed either by superoxide dismutase or spontaneously, to produce hydrogen peroxide. Hence, detection of intracellular hydrogen peroxide by PF1 probably indirectly reflects superoxide production in cells. As shown in the MTS results (Figure 2), HaCaT cells were almost completely killed by both (γ-CyD)$_2$/C_{60} and $C_{60}(OH)_{24}$ at concentrations of 0.5 and 30 μM, respectively. We selected the same conditions to measure the different levels of intracellular hydrogen peroxide (Figure 9). Confocal fluorescence microscopy clearly indicated a higher level of hydrogen peroxide production in cells incubated with $C_{60}(OH)_{24}$ upon illumination, again suggesting that the phototoxicity of $C_{60}(OH)_{24}$ is mediated by a type I photochemical pathway. Moreover, it should be pointed out that the fluorescence visible upon illumination of cells containing (γ-CyD)$_2$/C_{60} suggests that type I reactions also play a role in (γ-CyD)$_2$/C_{60} phototoxicity.

In conclusion, both (γ-CyD)$_2$/C_{60} and $C_{60}(OH)_{24}$ are phototoxic toward HaCaT cells. However, the phototoxicity of (γ-CyD)$_2$/C_{60} is greater than $C_{60}(OH)_{24}$. The phototoxicity of (γ-CyD)$_2$/C_{60} must initially involve a type II (singlet oxygen) reaction with type I (free radicals) reactions playing only a minor role. In contrary, $C_{60}(OH)_{24}$ phototoxicity mainly involves type I (free radical) reactions. Our findings indicate that fullerenes, especially (γ-CyD)$_2$/C_{60}, could potentially be used in photodynamic therapy to kill tumor cells. On the other hand, concern is also warranted about the use of fullerenes as a drug or drug carrier to treat normal cells.

Acknowledgment

This research was supported by the Intramural Research Program of the NIH, National Institute of Environmental Health Sciences. We are indebted to Dr. Ann Motten and Dr. Albert Wielgus, NIEHS, for critical reading of the manuscript.

References

(1). Bosi S, Da Ros T, Spalluto G, Prato M. Fullerene derivatives: An attractive tool for biological applications. Eur. J. Med. Chem 2003;38:913–923. [PubMed: 14642323]

(2). Wilson LJ, Cagle DW, Thrash TP, Kennel SJ, Mirzadeh S, Alford JM, Ehrhardt GJ. Metallofullerene drug design. Coord. Chem. Rev 1999;192:199–207.

(3). Da Ros T, Prato M. Medicinal chemistry with fullerenes and fullerene derivatives. Chem. Commun 1999:663–669.

(4). Gonzalez KA, Wilson LJ, Wu WJ, Nancollas GH. Synthesis and in vitro characterization of a tissue-selective fullerene: Vectoring C-60(OH)(16)AMBP to mineralized bone. Bioorg. Med. Chem 2002;10:1991–1997. [PubMed: 11937359]

(5). Sayes CM, Gobin AM, Ausman KD, Mendez J, West JL, Colvin VL. Nano-C-60 cytotoxicity is due to lipid peroxidation. Biomaterials 2005;26:7587–7595. [PubMed: 16005959]

(6). Oberdorster E. Manufactured nanomaterials (fullerenes, C-60) induce oxidative stress in the brain of juvenile largemouth bass. Environ. Health Perspct 2004;112:1058–1062.

(7). Sayes CM, Fortner JD, Guo W, Lyon D, Boyd AM, Ausman KD, Tao YJ, Sitharaman B, Wilson LJ, Hughes JB, West JL, Colvin VL. The differential cytotoxicity of water-soluble fullerenes. Nano Lett 2004;4:1881–1887.

(8). Lee J, Fortner JD, Hughes JB, Kim JH. Photochemical production of reactive oxygen species by C-60 in the aqueous phase during UV irradiation. Environ. Sci. Technol 2007;41:2529–2535. [PubMed: 17438811]

(9). Nakamura E, Isobe H. Functionalized fullerenes in water. The first 10 years of their chemistry, biology, and nanoscience. Acc. Chem. Res 2003;36:807–815. [PubMed: 14622027]

(10). Zhao B, Bilski PJ, He Y-Y, Feng L, Chignell CF. Photo-induced reactive oxygen species generation by different water-soluble fullerenes (C60) and their cytotoxicity in human keratinocytes. Photochem. Photobiol. 2008In press

(11). Nagano T, Arakane K, Ryu A, Masunaga T, Shinmoto K, Mashiko S, Hirobe M. Comparison of singlet oxygen production efficiency of C-60 with other photosensitizers, based on 1268-Nm emission. Chem. Pharm. Bull 1994;42:2291–2294.

(12). Sera N, Tokiwa H, Miyata N. Mutagenicity of the fullerene C60-generated singlet oxygen dependent formation of lipid peroxides. Carcinogenesis 1996;17:2163–2169. [PubMed: 8895484]

(13). Arbogast JW, Darmanyan AP, Foote CS, Rubin Y, Diederich FN, Alvarez MM, Anz SJ, Whetten RL. Photophysical properties of C60. J. Phys. Chem 1991;95:11–12.

(14). Nakanishi I, Ohkubo K, Fujita S, Fukuzumi S, Konishi T, Fujitsuka M, Ito O, Miyata N. Direct detection of superoxide anion generated in C-60-photosensitized oxidation of NADH and an analogue by molecular oxygen. J. Chem. Soc., Perkin Trans. 2 2002:1829–1833.

(15). Nakanishi I, Fukuzumi S, Konishi T, Ohkubo K, Fujitsuka M, Ito O, Miyata N. DNA cleavage via superoxide anion formed in photoinduced electron transfer from NADH to gamma-cyclodextrin-bicapped C-60 in an oxygen-saturated aqueous solution. J. Phys. Chem. B 2002;106:2372–2380.

(16). Yamakoshi Y, Umezawa N, Ryu A, Arakane K, Miyata N, Goda Y, Masumizu T, Nagano T. Active oxygen species generated from photoexcited fullerene (C60) as potential medicines: $O_2^{\cdot -}$ versus $^1O_2$. J. Am. Chem. Soc 2003;125:12803–12809. [PubMed: 14558828]

(17). Stasko A, Brezova V, Rapta P, Asmus KD, Guldi DM. [60]Fullerene anions in aqueous solutions (EPR study). Chem. Phys. Lett 1996;262:233–240.

(18). Yamakoshi Y, Sueyoshi S, Fukuhara K, Miyata N. $^{\cdot}OH$ and $O_2^{\cdot -}$ generation in aqueous C-60 and C-70 solutions by photoirradiation: An EPR study. J. Am. Chem. Soc 1998;120:12363–12364.

(19). Tokuyama H, Yamago S, Nakamura E, Shiraki T, Sugiura Y. Photoinduced biochemical-activity of fullerene carboxylic-acid. J. Am. Chem. Soc 1993;115:7918–7919.

(20). Deguchi S, Alargova RG, Tsujii K. Stable dispersions of fullerenes, C-60 and C-70, in water. Preparation and characterization. Langmuir 2001;17:6013–6017.

(21). Fortner JD, Lyon DY, Sayes CM, Boyd AM, Falkner JC, Hotze EM, Alemany LB, Tao YJ, Guo W, Ausman KD, Colvin VL, Hughes JB. C-60 in water: Nanocrystal formation and microbial response. Environ. Sci. Technol 2005;39:4307–4316. [PubMed: 15984814]

(22). Andrievsky GV, Kosevich MV, Vovk OM, Shelkovsky VS, Vashchenko LA. On the production of an aqueous colloidal solution of fullerenes. J. Chem. Soc., Chem. Commun 1995:1281–1282.

(23). Bensasson RV, Bienvenue E, Dellinger M, Leach S, Seta P. C60 in model biological systems—A visible-UV absorption study of solvent-dependent parameters and solute aggregation. J. Phys. Chem 1994;98:3492–3500.

(24). Yamakoshi YN, Yagami T, Fukuhara K, Sueyoshi S, Miyata N. Solubilization of fullerenes into water with polyvinylpyrrolidone applicable to biological tests. J. Chem. Soc., Chem. Commun 1994:517–518.

(25). Sawada H, Iidzuka J, Maekawa T, Takahashi R, Kawase T, Oharu K, Nakagawa H, Ohira K. Solubilization of fullerene into water with fluoroalkyl end-capped amphiphilic oligomers-novel fluorescence properties. J. Colloid Interface Sci 2003;263:1–3. [PubMed: 12804877]

(26). Terashima M, Nagao S. Solubilization of [60]fullerene in water by aquatic humic substances. Chem. Lett 2007;36:302–303.

(27). Gharbi N, Pressac M, Hadchouel M, Szwarc H, Wilson SR, Moussa F. [60]Fullerene is a powerful antioxidant in vivo with no acute or subacute toxicity. Nano Lett 2005;5:2578–2585. [PubMed: 16351219]

(28). Nishibayashi Y, Saito M, Uemura S, Takekuma S, Takekuma H, Yoshida Z. Buckminsterfullerenes—A non-metal system for nitrogen fixation. Nature 2004;428:279–280. [PubMed: 15029186]

(29). Yoshida ZI, Takekuma H, Takekuma SI, Matsubara Y. Molecular recognition of C-60 with gamma-cyclodextrin. Angew. Chem., Int. Ed 1994;33:1597–1599.

(30). Andersson T, Nilsson K, Sundahl M, Westman G, Wennerstrom O. C-60 embedded in gamma-cyclodextrin—A water-soluble fullerene. J. Chem. Soc., Chem. Commun 1992:604–606.

(31). Vileno B, Marcoux PR, Lekka M, Sienkiewicz A, Feher T, Forro L. Spectroscopic and photophysical properties of a highly derivatized C-60 fullerol. Adv. Funct. Mater 2006;16:120–128.

(32). Lamparth I, Hirsch A. Water-soluble malonic-acid derivatives of C-60 with a defined 3-dimensional structure. J. Chem. Soc., Chem. Commun 1994:1727–1728.

(33). Guldi DM, Hungerbuhler H, Asmus KD. Radiolytic reduction of a water-soluble fullerene cluster. J. Phys. Chem. A 1997;101:1783–1786.

(34). Sijbesma R, Srdanov G, Wudl F, Castoro JA, Wilkins C, Friedman SH, Decamp DL, Kenyon GL. Synthesis of a fullerene derivative for the inhibition of HIV enzymes. J. Am. Chem. Soc 1993;115:6510–6512.

(35). Delpeux S, Beguin F, Benoit R, Erre R, Manolova N, Rashkov I. Fullerene core star-like polymers—1. Preparation from fullerenes and monoazidopolyethers. Eur. Polym. J 1998;34:905–915.

(36). Chang MCY, Pralle A, Isacoff EY, Chang CJ. A selective, cell-permeable optical probe for hydrogen peroxide in living cells. J. Am. Chem. Soc 2004;126:15392–15393. [PubMed: 15563161]

(37). Hall RD, Chignell CF. Steady-state near-infrared detection of singlet molecular-oxygen—A Stern-Volmer quenching experiment with sodium-azide. Photochem. Photobiol 1987;45:459–464. [PubMed: 3575442]

(38). Bilski P, Chignell CF. Optimization of a pulse laser spectrometer for the measurement of the kinetics of singlet oxygen O-2(Delta(1)(g)) decay in solution. J. Biochem. Biophys. Methods 1996;33:73–80. [PubMed: 8951528]

(39). Bilski P, Martinez LJ, Koker EB, Chignell CF. Photosensitization by norfloxacin is a function of pH. Photochem. Photobiol 1996;64:496–500. [PubMed: 8806228]

(40). Boukamp P, Petrussevska RT, Breitkreutz D, Hornung J, Markham A, Fusenig NE. Normal keratinization in a spontaneously immortalized aneuploid human keratinocyte cell line. J. Cell Biol 1988;106:761–771. [PubMed: 2450098]

(41). Wright A, Hawkins CL, Davies MJ. Photo-oxidation of cells generates long-lived intracellular protein peroxides. Free Radical Biol. Med 2003;34:637–647. [PubMed: 12633741]

(42). Guldi DM, Hungerbuhler H, Asmus KD. Unusual redox behavior of a water-soluble malonic-acid derivative of C-60—Evidence for possible cluster formation. J. Phys. Chem 1995;99:13487–13493.

(43). Guldi DM, Hungerbuhler H, Asmus KD. Redox and excitation studies with C-60-substituted malonic-acid diethyl esters. J. Phys. Chem 1995;99:9380–9385.

(44). Ji ZQ, Sun HF, Wang HF, Xie QY, Liu YF, Wang Z. Biodistribution and tumor uptake of C-60 (OH)(x) in mice. J. Nanopart. Res 2006;8:53–63.

(45). Mohan H, Palit DK, Mittal JP, Chiang LY, Asmus KD, Guldi DM. Excited states and electron transfer reactions of C-60(OH)(18) in aqueous solution. J. Chem. Soc., Faraday Trans 1998;94:359–363.

(46). He YY, Huang JL, Ramirez DC, Chignell CF. Role of reduced glutathione efflux in apoptosis of immortalized human keratinocytes induced by UVA. J. Biol. Chem 2003;278:8058–8064. [PubMed: 12502708]

(47). Davies MJ, Hawkins C, Wright A. Singlet oxygen-mediated formation of protein peroxides within cells. Free Radical Biol. Med 2002;33:S420–S420.

(48). Kochevar IE, Bouvier J, Lynch M, Lin CW. Influence of dye and protein location on photosensitization of the plasma-membrane. Biochim. Biophys. Acta-Biomembr 1994;1196:172–180.

(49). Wilkinson F, Helman WP, Ross AB. Rate constants for the decay and reactions of the lowest electronically excited singlet-state of molecular-oxygen in solution—An expanded and revised compilation. J. Phys. Chem. Ref. Data 1995;24:663–1021.

(50). Kamat JP, Devasagayam TP, Priyadarsini KI, Mohan H. Reactive oxygen species mediated membrane damage induced by fullerene derivatives and its possible biological implications. Toxicology 2000;155:55–61. [PubMed: 11154797]

(51). Petrat F, Pindiur S, Kirsch M, de Groot H. NAD(P)H, a primary target of 1O2 in mitochondria of intact cells. J. Biol. Chem 2003;278:3298–3307. [PubMed: 12433931]

(52). Moan J. On the diffusion length of singlet oxygen in cells and tissues. J. Photochem. Photobiol. B, Biol 1990;6:343–347.

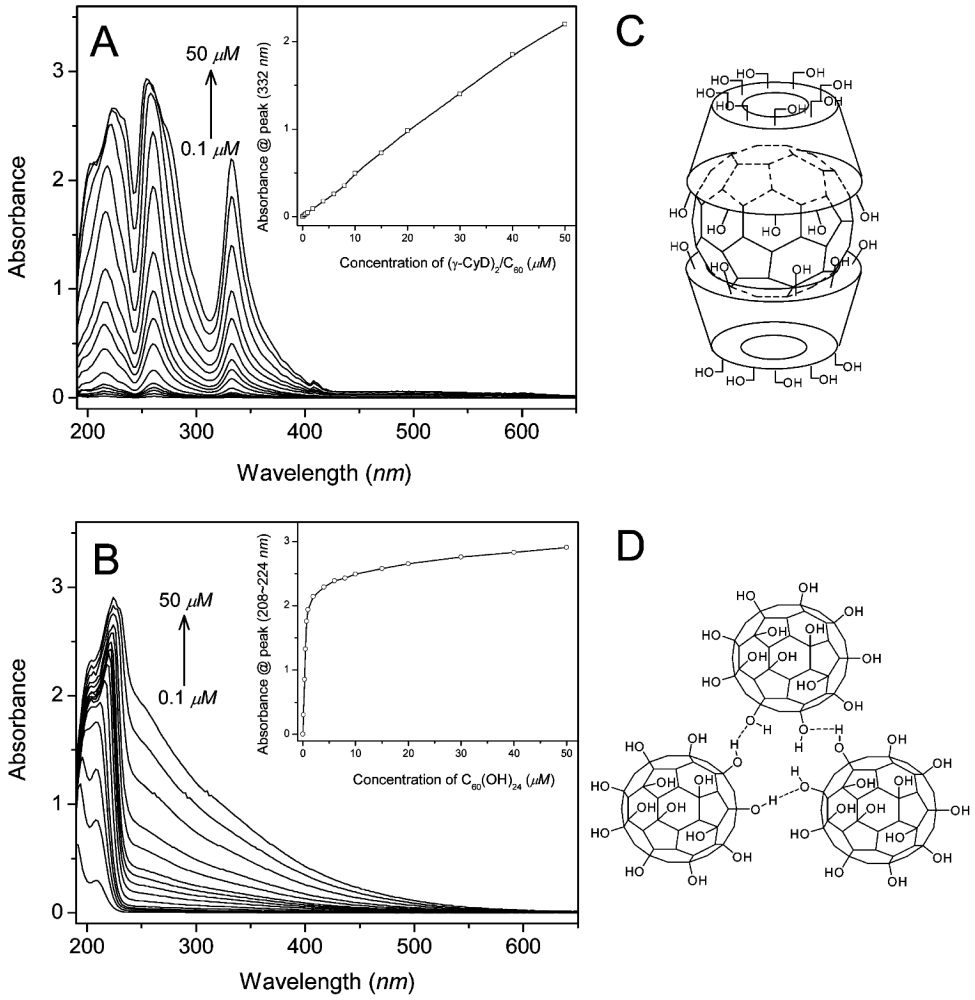

Figure 1.

(A) UV-vis absorption spectra of different concentrations of $(\gamma\text{-CyD})_2/C_{60}$ and (B) $C_{60}(OH)_{24}$ in aqueous solution. Spectra from bottom to top correspond to $[(\gamma\text{-CyD})_2/C_{60}]$ or $[C_{60}(OH)_{24}]$ = 0.1, 0.3, 0.5, 0.7, 1, 2, 4, 6, 8, 10, 15, 20, 30, 40, and 50 μM. Inset: Plot of the peak absorbance against the concentration; path length, 1 cm. (C) Structure of $(\gamma\text{-CyD})_2/C_{60}$. (D) Possible structure of $C_{60}(OH)_{24}$ aggregates in aqueous solution.

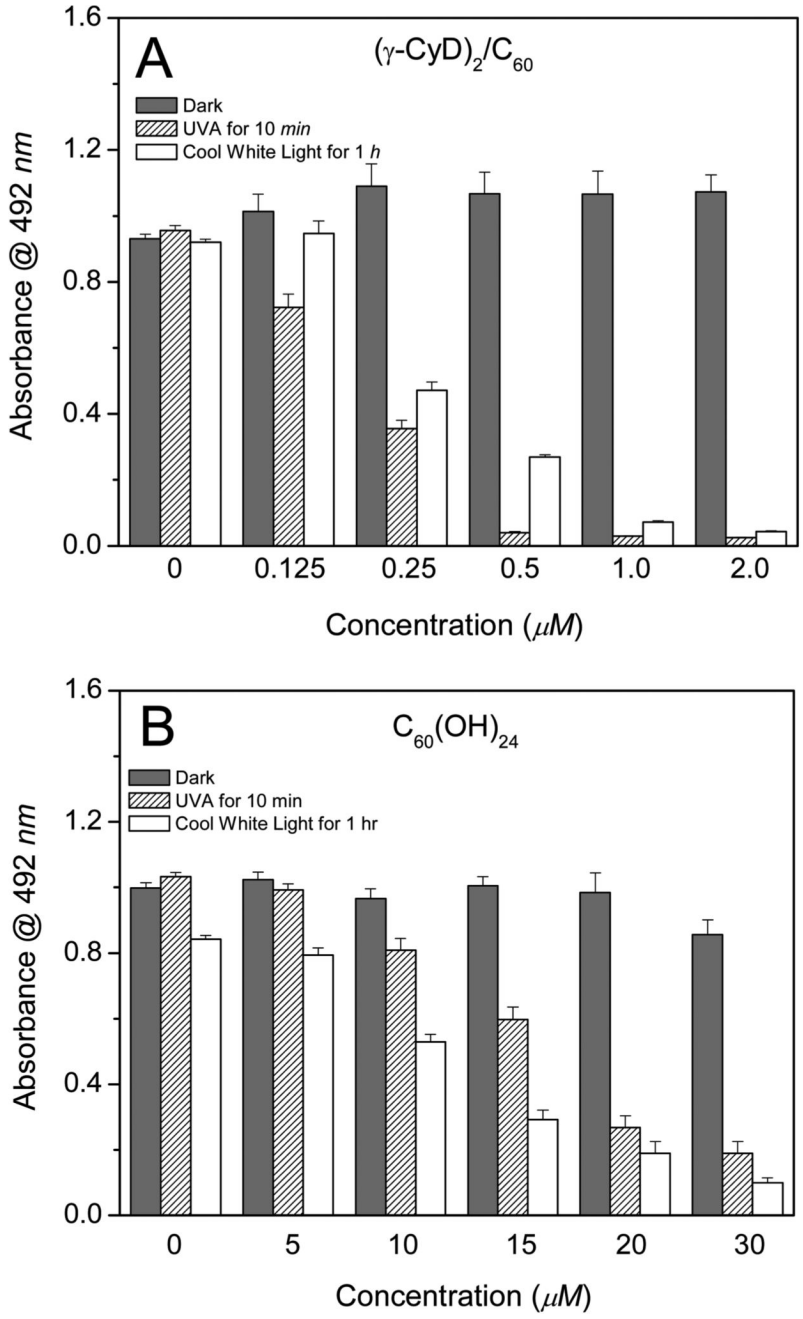

Figure 2.

(A) Effect of (γ-CyD)$_2$/C$_{60}$ and (B) C$_{60}$(OH)$_{24}$ exposure on the viability of HaCaT keratinocytes irradiated with UVA (15 J/cm^2) and cool white light (5.4 J/cm (2)) as measured by the MTS assay (see the Materials and Methods). Values are the means ± SE (n = 8).

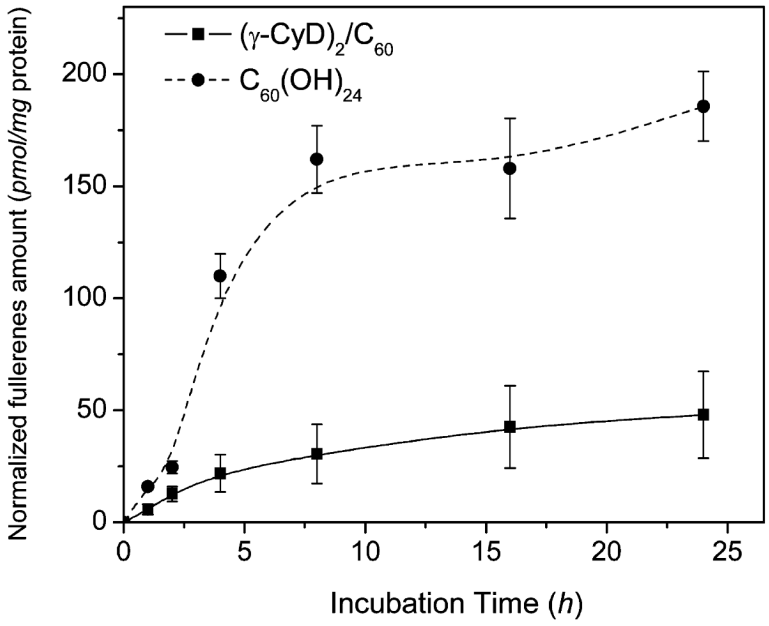

Figure 3.

Uptake of (γ-CyD)$_2$/C$_{60}$ and C$_{60}$(OH)$_{24}$ by HaCaT keratinocytes. The cells were incubated in the dark in DMEM containing 50 μM (γ-CyD)$_2$/C$_{60}$ or C$_{60}$(OH)$_{24}$. The amount of fullerenes in cells was determined spectrophotometrically and normalized to the concentration of protein.

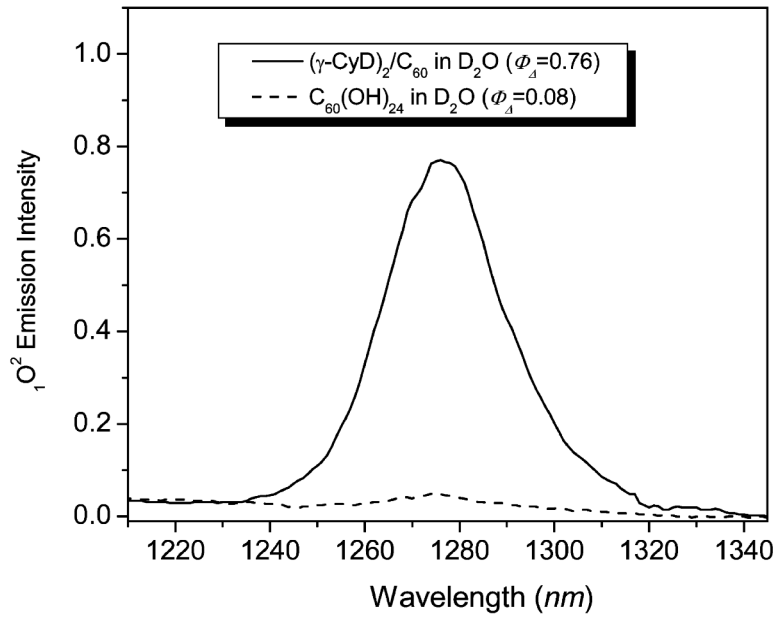

Figure 4.
Steady state near-infrared $^1O_2$ phosphorescence emission spectra of (γ-CyD)$_2$/C_{60} and $C_{60}(OH)_{24}$ in D_2O (λ_{ex} = 366 nm).

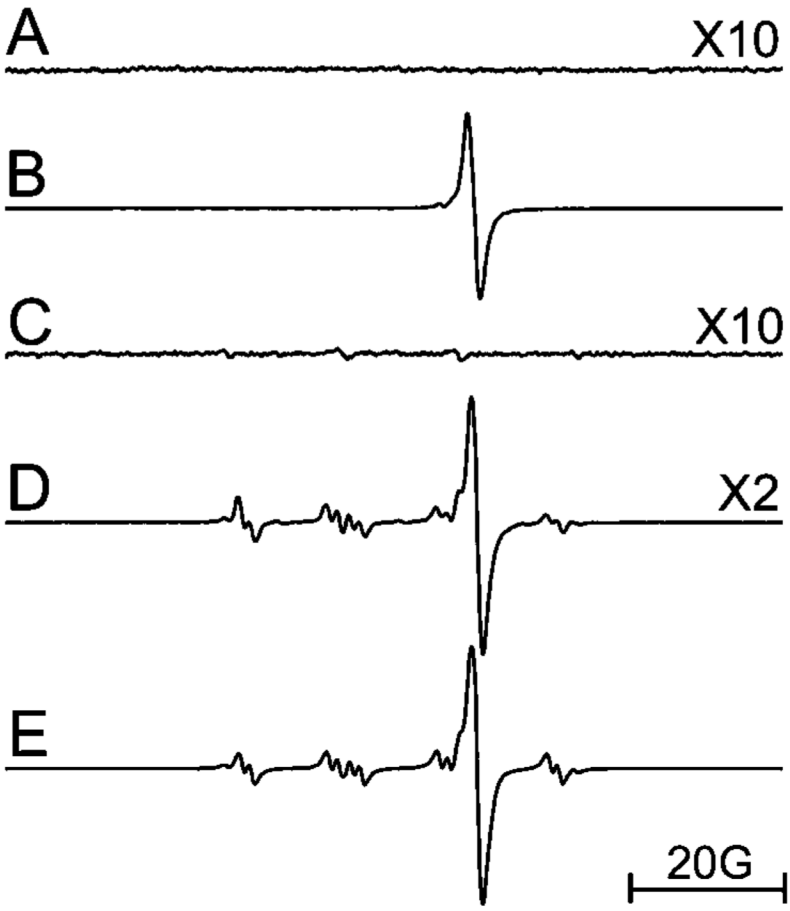

Figure 5.

EPR spectra of an aqueous solution of (γ-CyD)$_2$/C_{60} (50 μM). (A) Irradiated (λ > 300 nm); (B) irradiated (λ > 300 nm) in the presence of 5 mM NADH; (C) irradiated (λ > 400 nm) in the presence of 80 mM DMPO; (D) same as part C with the addition of 5 mM NADH; and (E) simulation of part D using the following parameters: DMPO/$O_2^{\cdot-}$ (a_N = 14.1 G, a_{H1} = 11.3 G, and a_{H2} = 1.2 G; 41.7%), (γ-CyD)$_2$/$C_{60}^{\cdot-}$ (0.97 G line width and +10.8 G *g* shift; 55.3%), DMPO/$^{\cdot}$OH (a_N = 15.0 G and a_H = 14.9 G; 3.0%). Instrumental settings: microwave power, 10 mW; modulation frequency, 100 kHz; modulation amplitude, 1 G; time constant, 655 ms; 335 s scan time; and scan range, 100 G.

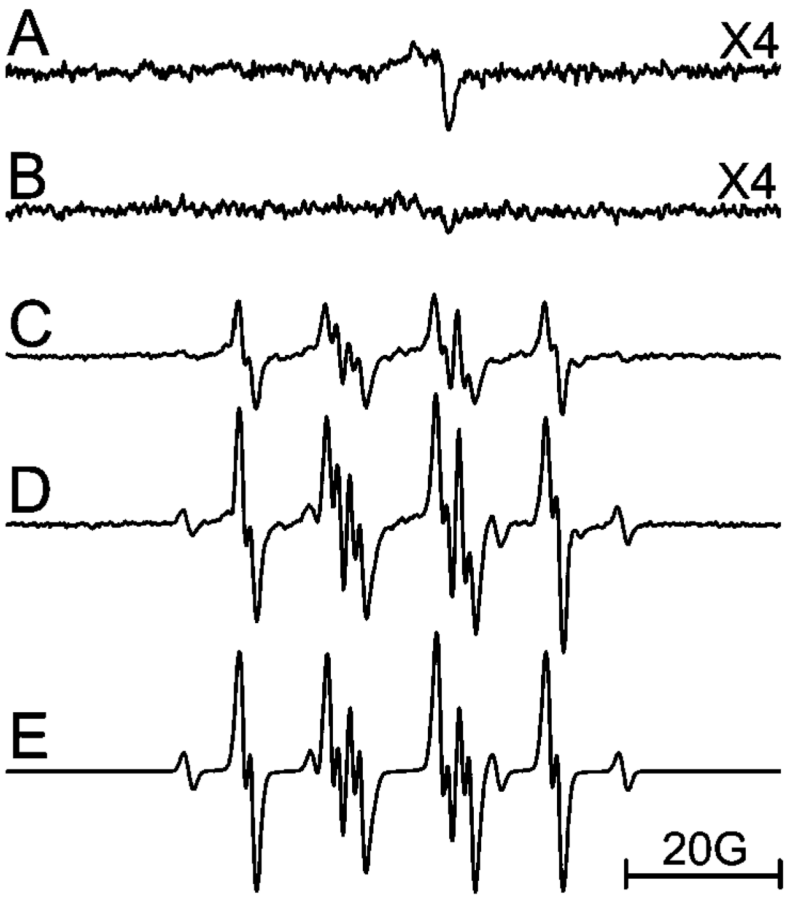

Figure 6.

EPR spectrum of an aqueous solution of $C_{60}(OH)_{24}$ (50 μM) containing 1% DMSO. (A) Irradiated (λ > 300 nm); (B) irradiated (λ > 300 nm) in the presence of 5 mM NADH; (C) irradiated (λ > 400 nm) in the presence of 80 mM DMPO; (D) same as part C with the addition of 5 mM NADH; and (E) simulation of part D using the following parameters: DMPO/$O_2^{\cdot-}$ (a_N = 14.1 G, a_{H1} = 11.3 G, and a_{H2} = 1.2 G; 92.9%); DMPO/C$^{\cdot}$ (a_N = 16.3 G and a_H = 23.4 G; 7.1%). Instrumental settings: microwave power, 10 mW; modulation frequency, 100 kHz; modulation amplitude, 1 G; time constant, 655 ms; 335 s scan time; and scan range, 100 G.

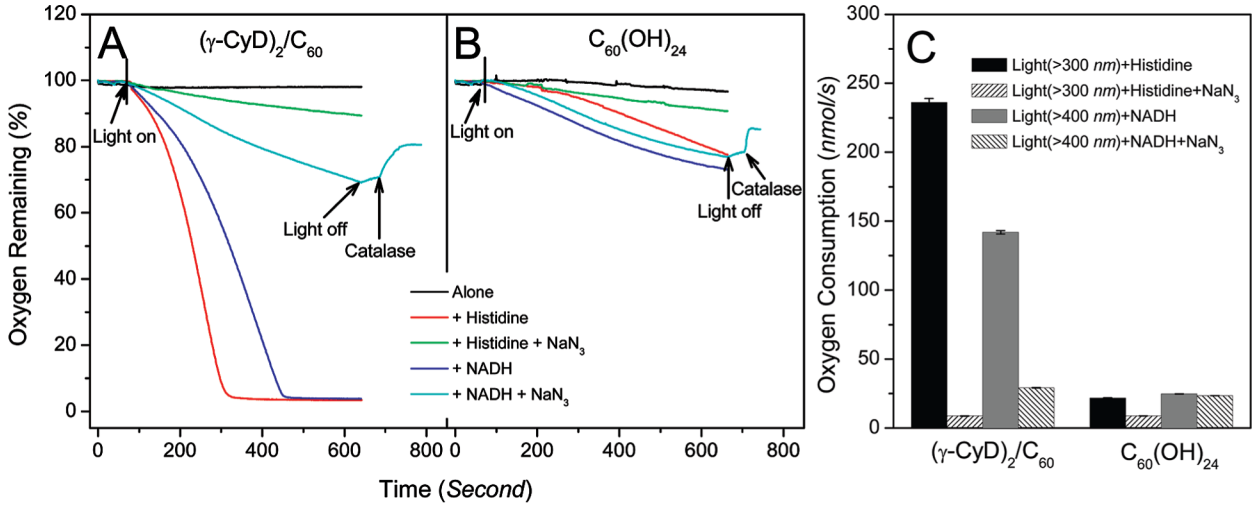

Figure 7.

(A) Oxygen consumption during illumination of 20 μM (γ-CyD)$_2$/C$_{60}$ and (B) C$_{60}$(OH)$_{24}$ in the absence or presence of 2 mM histidine or NADH with or without 10 mM sodium azide in water. Catalase (50 μg/mL) was added where indicated. (C) Oxygen consumption rates (nmol/s) for (γ-CyD)$_2$/C$_{60}$ and C$_{60}$(OH)$_{24}$ as shown in parts A and B.

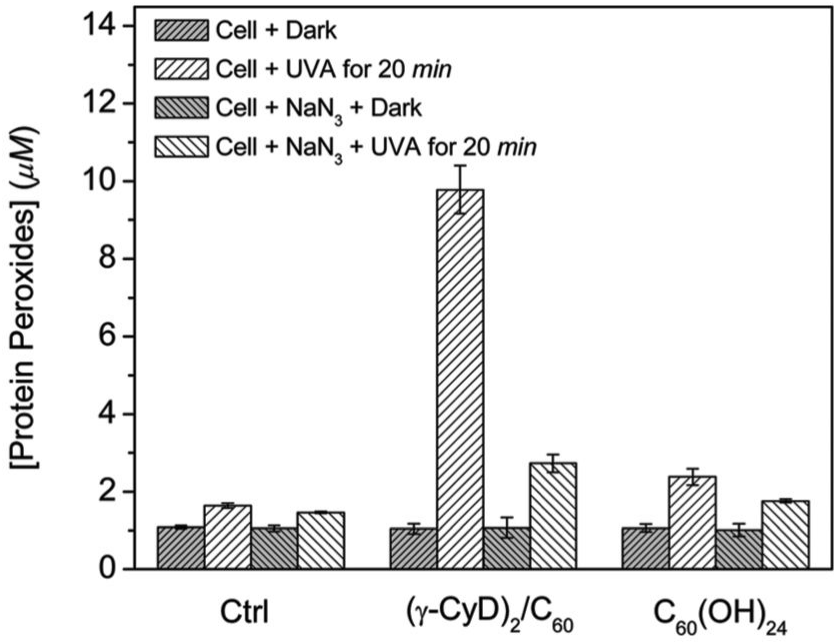

Figure 8.

Effect of $(\gamma\text{-CyD})_2/C_{60}$ and $C_{60}(OH)_{24}$ exposure on the formation of protein peroxides during illumination of HaCaT cells in the absence or presence of 10 mM sodium azide. Cells (4×10^6 cells mL^{-1}) were incubated with 10 μM $(\gamma\text{-CyD})_2/C_{60}$ or $C_{60}(OH)_{24}$ for 2 h before illumination with UVA (15 J/cm^2) for 20 min.

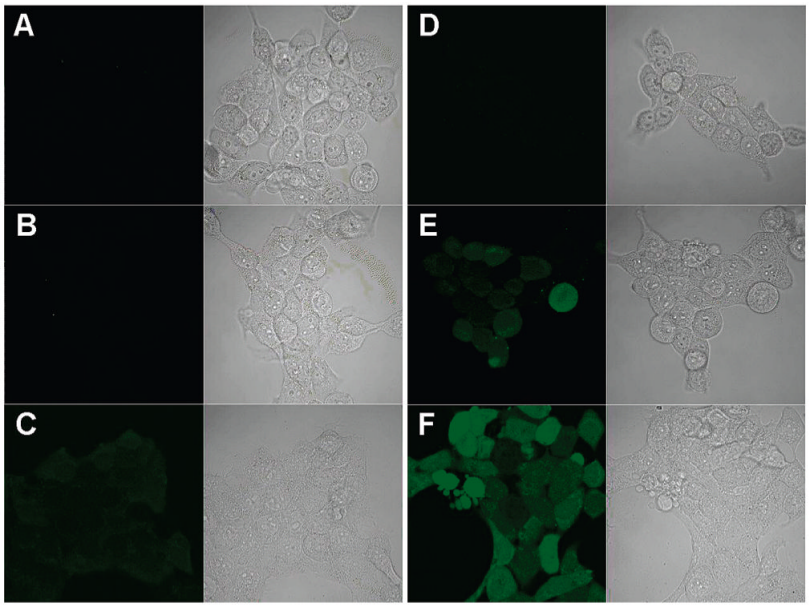

Figure 9.

Confocal images of HaCaT cells stained with 5 μM PF1; ex/em, 488/505-550 nm. (A) Cells were kept in the dark and incubated with 5 μM PF1 for 5 min at RT; left, confocal fluorescence microscopy; right, brightfield transmission microscopy. (B) Same as part A except that cells were incubated with 0.5 μM (γ-CyD)$_2$/C_{60} for 2 h at 37 °C before staining with PF1. (C) Same as part B except that cells were incubated with 30 μM $C_{60}(OH)_{24}$. (D-F) Same as parts A-C, respectively, except that cells were then exposed to UVA (15 J/cm^2) for 10 min.

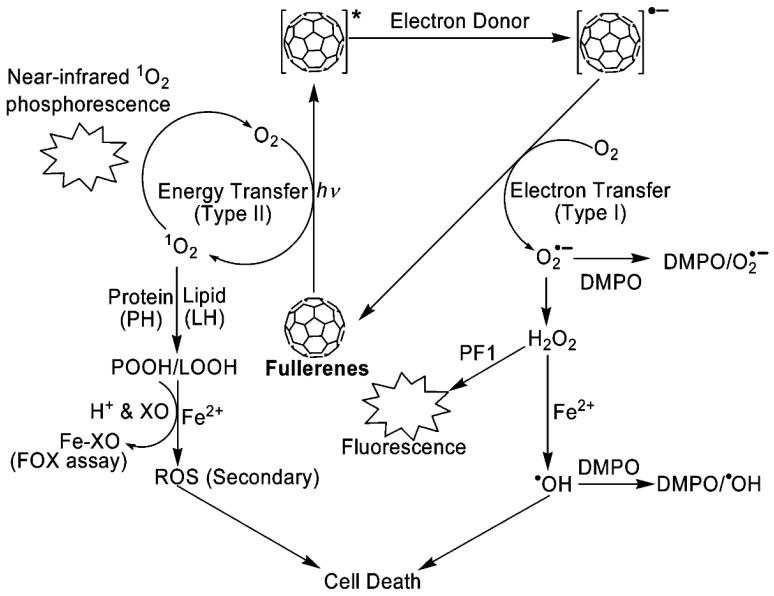

Scheme 1.